Memory effects in the frictional damping of diffusive and vibrational motion of adatoms

A. Cucchetti and S. C. Ying
Department of Physics, Brown University, Box 1843, Providence, Rhode Island 02906
(Received 15 November 1995)

We investigate the memory effects in the frictional damping of the vibrational and diffusive motion of an adatom. Using the molecular-dynamics simulation method, we solve the equations of motion of an adatom in a periodic potential coupled to substrate phonons which are in turn coupled to a heat bath. The frustrated translational mode and the diffusion constant of the adatom is studied by calculating appropriate time-dependent correlation functions. We discuss our numerical results in the context of a generalized Langevin equation. The validity of analytic approximations to the memory function in the Langevin equation such as mode-mode coupling and initial value approximation are examined by comparing the analytic results with those obtained from the numerical simulations. [S0163-1829(96)02229-1]

I. INTRODUCTION

Much attention has recently been focused on the dynamical properties of adatoms coupled to substrate excitations. The diffusive as well as the vibrational motion of the adsorbate have been probed with several experimental techniques.[1–3] Theoretical models have also been developed to explain the process of diffusion[1,4–9] and the different mechanisms that affect the vibrational properties of the adatom.[3,10–14]

Most of these theoretical studies have focused on physical systems where the substrate excitation time scale is much shorter than the time scale of the motion of the adatom. In this case, memory effects are not important and the motion of the adsorbate is described by a simple Langevin equation with a damping force proportional to the instantaneous velocity.[6,15–19] If, however, the excitations have a time scale comparable, or longer than that of the adatom, then the process is non-Markovian and memory effects become important.[20–26]

In this paper, we investigate the mechanism of the adatom-phonons coupling and its effect on the diffusive and vibrational properties of the adatom using molecular-dynamics (MD) simulation studies. Our object is to understand in detail the memory effects in the frictional damping of the adatom due to the coupling to the substrate phonon excitations. In particular, we study a coupling which is nonlinear in the adatom coordinates, and we stress the differences and similarities with the more commonly studied linear coupling case. The nonlinear effects are most important in the temperature range of the order of the energy barrier. In this regime the diffusive and vibrational motion of the adatom are intrinsically coupled to each other; so they cannot be studied separately.[22–24] In our model, therefore, diffusive and vibrational motion are treated on equal footing. Experimentally this regime can be probed using the helium scattering technique.[27–29] We calculate the diffusion constant as well as the width and the shift of the frustrated translational mode. The physical mechanisms responsible for the broadening of the vibrational peak are clarified through the study of the energy as well as the velocity autocorrelation function for the adatom. The results are analyzed in three different regimes: $\omega_D \gg \omega_0$, $\omega_D \simeq \omega_0$, and $\omega_D \ll \omega_0$, where ω_D is the maximum frequency of the substrate excitations, while ω_0 is the characteristic vibrational frequency of the adatom. In the case of $\omega_D \gg \omega_0$, we recover the results obtained earlier analytically.[24] In the other regimes, $\omega_D \simeq \omega_0$ and $\omega_D \ll \omega_0$, the vibrational and diffusive motion of the adatom is strongly influenced by the nonlinearity of the coupling. No exact analytical results exist in this case.

Formally, the motion of the substrate phonons can be integrated out and the adatom motion can then be described by a generalized Langevin equation (GLE) with a memory function replacing the simple damping described by a constant friction,[16,17,30–33] However, even though a formal expression for the memory function can be obtained, in most cases the detailed evaluation of the memory function is not possible. Moreover, for a general memory function, no analytic solution of the GLE valid in all the frequency regimes exists. In the literature, two main approximations for the memory function have been used.[20–22,24] The first one is the initial value approximation (IVA). Here, the adatom time scale is assumed to be much longer than the substrate vibrational period and the adatom coordinate in the memory function is therefore replaced by its initial value. This results in a memory function similar to the linear coupling case and allows an analytic solution for the various correlation functions using a matrix continued-fraction method.[16,17,24,30,31] For the cases where the two time scales are comparable and a clear cut separation is not possible, the mode-mode coupling approximation is often employed. This involves the factorization of the memory function into the product of two time correlation functions, one for the adatom motion, and the other for the substrate motion. The various time correlation functions for the adatom can then be determined self-consistently. In this paper, besides studying the dynamics of the adatom for our theoretical model through molecular-dynamics simulation, we also solve the corresponding GLE using these standard approximations for the memory function. This allows us to compare the analytic and numerical approaches to establish the region of validity, if any, of these standard approximations widely used in the literature.

II. THE MODEL

Since our main interest is to explore the qualitative feature of nonlinear coupling to the substrate and memory ef-

fects in the frictional damping, in this paper, we adopt the simplest theoretical model which contains all the necessary ingredients. First of all, we restrict the motion of the adatom to one dimension. The extension to higher dimension is straightforward. The substrate excitations, however, are still fully three dimensional. We describe an adatom interacting with substrate excitations with the following Hamiltonian:

$$H = H_{\rm ph} + H_0 + H_{\rm int}. \tag{2.1}$$

There are three components in this Hamiltonian. The first part is the Hamiltonian for the substrate excitations in the harmonic approximation:

$$H_{\rm ph} = \sum_{\lambda} \left[\frac{p_\lambda^2}{2M} + \frac{M\omega_\lambda^2}{2} u_\lambda^2 \right]. \tag{2.2}$$

This describes the substrate by a set of harmonic oscillators corresponding to the normal modes of the lattice characterized by an index λ. The frequency, coordinate and momenta of the normal mode are denoted by ω_λ, u_λ, and p_λ, respectively.

The second part describes an adatom in a static potential:

$$H_0 = \frac{p^2}{2m} + V(x) + \sum_{\lambda} \frac{M\omega_\lambda^2}{2} W_\lambda^2(x), \tag{2.3}$$

where x and p are the adatom position and momentum, m and M are the adatom and the substrate atom masses, respectively, $V(x)$ is the static potential, and $W_\lambda(x)$ is a function describing the coupling of the adatom coordinate to the substrate excitations. Here the second term has been added in order to counterbalance the effect of the adiabatic force due to the coupling.[34] This way, the energy shift of the vibrational peak and the change in diffusion barrier are only due to the nonadiabatic effect of the adatom-phonons coupling.

Finally there is the coupling term

$$H_{\rm int} = \sum_{\lambda} \frac{M\omega_\lambda^2}{2} u_\lambda W_\lambda(x), \tag{2.4}$$

where each phonon mode is coupled to the adatom through the function $W_\lambda(x)$ that depends, in general, on the position of the adatom and on the particular phonon mode λ.

The force acting on the adatom is

$$\dot{p} = -\frac{d\widetilde{V}(x)}{dx} - \sum_{\lambda} \frac{M\omega_\lambda^2}{2} u_\lambda \frac{dW_\lambda(x)}{dx}, \tag{2.5}$$

where

$$\widetilde{V}(x) = V(x) + \sum_{\lambda} \frac{M\omega_\lambda^2}{2} W_\lambda^2(x).$$

There are two components in the force: the adiabatic part generated by the interaction with the substrate atoms on the lattice in their average position and the nonadiabatic part which is entirely due to fluctuations of the lattice and is responsible for the dissipation.

In this paper, we consider only coupling to substrate phonons and not to high-frequency excitations such as electron-hole pairs. The time scales for the electronic processes are much shorter than that of the adatom motion and clearly memory effects, in electronic friction, can be neglected. They can be easily included as an additional Markovian friction acting on the adatom.

The phonons are assumed to be in contact with a heat bath at a constant temperature. The coupling of the phonons to the heat bath are mathematically described by a Langevin equation with damping γ_λ and random force r_λ, related by the fluctuation and dissipation theorem:[40,41]

$$\langle r_\lambda(t) r_\lambda(t') \rangle = 2mk_B T \gamma_\lambda \delta(t-t'). \tag{2.6}$$

Therefore, in the absence of the adatom, the phonons behave like Brownian harmonic oscillators whose position correlation functions are known.[35,42] The adatom, instead, is only directly coupled to the phonons which thermalize its motion.

We choose for the adiabatic periodic surface potential the simplest cosine potential $V(x) = V_0[1-\cos(x/d)]$, where $d = a/2\pi$ and a is the lattice constant. For the phonons, we divide them into two groups according to their symmetries. The general index λ can now be replaced by the index (i,l) where $i = 1,2$ labels the symmetry group and l runs from 1 to $N/2$, with N being the total numbers of phonons considered. The frequencies ω_l have been chosen so that they depend only on the index l and not on the particular symmetry group. The coupling function is chosen to have the form $W_{1,l}(x) = \alpha V_0/(d\sqrt{N/2}M\omega_l^2)\sin(x/d)$ and $W_{2,l}(x) = \alpha V_0/(d\sqrt{N/2}M\omega_l^2)\cos(x/d)$ (see the Appendix for a discussion on the choice of this form of the coupling function). Here α is dimensionless and characterizes the coupling strength.

The equation of motion of the adatom is

$$\ddot{x} = -\frac{V_0}{md}\sin(x/d) - \frac{\alpha V_0}{md^2\sqrt{N/2}} \times \sum_{l=1}^{N/2} [u_{1,l}\cos(x/d) - u_{2,l}\sin(x/d)]. \tag{2.7}$$

The equations of motion for the phonon variables are

$$\ddot{u}_{1,l} = -\omega_l^2 u_{1,l} - \frac{\alpha V_0}{Md\sqrt{N/2}}\sin(x/d) - \gamma_l \dot{u}_{1,l} + \frac{r_l}{M},$$

$$\ddot{u}_{2,l} = -\omega_l^2 u_{2,l} - \frac{\alpha V_0}{Md\sqrt{N/2}}\cos(x/d) - \gamma_l \dot{u}_{2,l} + \frac{r_l}{M}, \tag{2.8}$$

where γ_l is a constant friction and r_l is the corresponding random force.

The dynamics of the adatom can be easily studied by evaluating appropriate time-dependent correlation functions. The Fourier transform of the velocity autocorrelation function of the adatom is defined as

$$D(\omega) \equiv \int_{-\infty}^{+\infty} e^{-i\omega t} \langle v(t)v(0) \rangle dt. \tag{2.9}$$

This correlation function yields important information on the dynamical processes on the surface: at finite frequency $D(\omega)$ describes the vibrational spectrum of the adatom while

its zero-frequency limit $D(0)$ is exactly twice the diffusion constant.[1,5] In order to understand the different mechanism responsible for broadening of the vibrational peak, we also evaluate the Fourier transform of the energy autocorrelation function:

$$E(\omega)\equiv\int_{-\infty}^{+\infty}e^{-i\omega t}\langle(E(t)-\langle E(t)\rangle),E(0)\rangle dt, \quad (2.10)$$

where $E=p^2/2m+V_0[1-\cos(x/d)]$ and $\langle E(t)\rangle$ is the average value of the adatom energy at equilibrium. The Fourier transform of the energy autocorrelation function has a Lorentzian peak centered at zero. The width of the peak is a measure of the rate of energy transfer between the adatom and the substrate excitations, due to inelastic collisions between the phonons and the adatom. In the quantum limit, this is related to the inverse of the lifetime T_1 of the vibrational level. The study of the energy autocorrelation function thus allows us to separate the energy decay contribution to the broadening of the vibrational peak from pure dephasing mechanisms that also induce broadening.[10,43–45] These include the anharmonicity of the cosine potential and dephasing due to elastic scattering between adatom and phonons.

The damping effects of the substrate phonons on the adatom depends crucially on the function $\eta(t)$ which is essentially the correlation function of the phonon coordinates multiplied by the coupling constant α^2 and appropriately normalized:

$$\eta(t)=\frac{\alpha^2\beta V_0^2}{md^4}\frac{1}{N}\sum_{\lambda}\langle\tilde{u}_\lambda(t)\tilde{u}_\lambda(0)\rangle. \quad (2.11)$$

Here $\tilde{u}_\lambda(t)$ describes the time dependence of the particular phonon mode in the absence of the adatom, and β is the inverse of the thermal energy. As we will show in the next section, $\eta(t)$ is related to the frictional damping generated by the adatom-phonons coupling. In the special case of linear coupling, it is exactly the memory function appearing in the generalized Langevin equation. Examining (2.11), one sees that in the thermodynamic limit $\eta(t)$ depends only on the density of state per unit volume $\rho(w)$ and not on any other details of the phonon excitations. Equation (2.11) in this limit can be written as

$$\eta(t)=\frac{\alpha^2V_0^2}{mMd^4}\frac{\Omega_0}{N}\int_0^{+\infty}\frac{\rho(\omega)}{\omega^2}\cos(\omega t)d\omega. \quad (2.12)$$

Here Ω_0 is the volume and $\rho(\omega)$ is the density of states per unit volume. Thus, instead of actually using macroscopically large number of phonons in our simulation, we need only to deal with a small number of ''effective'' phonons.[42] The effect on the adatom motion due to the coupling to these effective phonons would be identical to the real macroscopic system provided that the damping and the frequency of these effective phonons are chosen to generate the same density of states as the actual macroscopic number of phonons. It will be shown below that, even for nonlinear coupling, the memory function in the initial value approximation or mode-mode coupling approximation is still proportional to $\eta(t)$. In this paper, the frequency ω_l and the damping γ_l of the phonon modes are chosen so that the resulting $\rho(\omega)$ and $\eta(\omega)$, fit, as closely as possible, to the corresponding functions in the Debye model for the substrate phonons. This is the simplest model for the substrate excitations that allows for the dispersion of the phonons and provides a time scale for the excitations in terms of the inverse of the cutoff frequency ω_D. It also allows us to compare the result of our simulation studies with earlier analytical studies[24] employing the same model for the substrate excitations. In the three-dimensional Debye model, the density of states $\rho(\omega)$ is given by the expression

$$\rho(\omega)=\frac{3\omega^2}{2\pi^2c^3}\Theta(\omega_D-\omega). \quad (2.13)$$

Here, c is the velocity of sound and ω_D is the Debye frequency. The real and imaginary part of the Laplace transform of $\eta(t)$, defined as

$$\eta(\omega)=\int_0^{+\infty}e^{i\omega t}\eta(t)dt, \quad (2.14)$$

can be evaluated easily to yield the result

$$\mathrm{Re}\,\eta(\omega)=\eta\Theta(\omega-\omega_D), \quad \mathrm{Im}\,\eta(\omega)=-\frac{\eta}{2\pi}\ln\left|\frac{\omega-\omega_D}{\omega+\omega_D}\right|, \quad (2.15)$$

and the constant η is

$$\eta=\frac{3\alpha^2V_0^2\Omega_0}{4\pi mc^3MNd^4}. \quad (2.16)$$

For our model with a finite number of modes, the function $\eta(t)$ can be expressed as

$$\eta(t)=\frac{\alpha^2\beta V_0^2}{md^4}\frac{2}{N}\sum_{l}^{N/2}\langle\tilde{u}_l(t)\tilde{u}_l(0)\rangle, \quad (2.17)$$

where the summation over λ is replaced by the one over l. The Laplace transform of $\eta(t)$ can be derived from the equations of motion (2.8) and

$$\eta(\omega)=\frac{\alpha^2V_0^2}{d^4Mm}\frac{2}{N}\sum_{l=1}^{N/2}\frac{1}{\omega_l^2}\frac{-i\omega+\gamma_l}{-\omega^2+\omega_l^2-i\omega\gamma_l}. \quad (2.18)$$

To mimic the Debye model, we choose the phonon parameters such that the real part of $\eta(\omega)$ approximates a step function as shown in Eq. (2.15). In Fig. 1 we plot the function $\mathrm{Re}\,\eta(\omega)$, resulting from our choice of $m=M=1$ and nine distinct phonon modes. The maximum phonon frequency in our model can be regarded as the effective Debye frequency ω_D which in Fig. 1 has chosen to be equal to ω_0. The approximation to the step function is reasonably good. The value of $\eta(\omega)$ at $\omega=0$ corresponds to the constant η in the Debye model result in (2.15).

III. GLE AND THE MEMORY FUNCTION

The motion of the adatom in our model can be equivalently described by a generalized Langevin equation[16,17,20,30,31]

$$\dot{p}+\frac{dV(x)}{dx}+\int_0^t\Sigma(t-t')p(t')dt'=R(t). \quad (3.1)$$

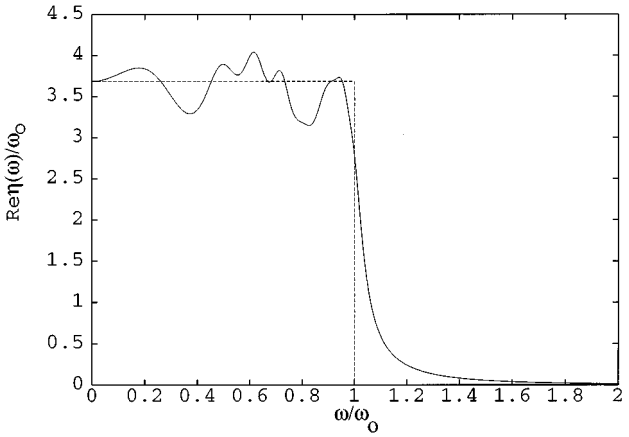

FIG. 1. $\mathrm{Re}\,\eta(\omega)/\omega_0$ vs ω/ω_0, with $\alpha=1$, $m=M=1$, and $\omega_D=\omega_0$.

Here, $R(t)$ is the nonadiabatic fluctuating random force. It is formally given by the expression $R(t)=\exp(-iQLQt)QLp$, with L the Liouville operator and Q the projection operator onto the Hilbert space orthogonal to adatom variables. The term QLp represents the nonadiabatic part of the force (2.5) (Ref. 24)

$$QLp=\sum_{\lambda} u_\lambda f_\lambda(x), \tag{3.2}$$

where $f_\lambda(x)\equiv M\omega_\lambda^2[dW_\lambda(x)/dx]$. For the coupling model adopted in this paper, we replace the general index λ by (i,l), and the coupling functions can be written as

$$f_{1,l}(x)=f_1(x)=\frac{\alpha V_0}{d^2\sqrt{N/2}}\cos(x/d),$$

$$f_{2,l}(x)=f_2(x)=\frac{-\alpha V_0}{d^2\sqrt{N/2}}\sin(x/d). \tag{3.3}$$

Note that, for this particular choice, the coupling is independent of the phonon index l.

The operator $\exp(-iQLQt)$ ensures that the time evolution of QLp is at all times orthogonal to the Hilbert space of the adatom variables. The memory function $\Sigma(t-t')$ is related to the fluctuating random force $R(t)$ by the fluctuation-dissipation theorem:

$$\langle R(t),R(t')\rangle=mk_BT\Sigma(t-t'). \tag{3.4}$$

So, using the definition of $R(t)$ and the relation (3.4), the memory function becomes

$$\Sigma(t)=\frac{\beta}{m}\sum_{\lambda}\langle u_\lambda f_\lambda(x)|\exp(iQLQt)|u_\lambda f_\lambda(x)\rangle. \tag{3.5}$$

This expression for the memory function is formal and does not allow easy evaluation. Thus, various approximations have been introduced. The exception is the case of linear coupling. For a constant $f_\lambda(x)=\alpha V_0/d^2\sqrt{N}$, the corresponding memory function is independent of the particle motion. The Liouville operator QLQ has the effect of projecting out the adatom coordinate in the phonons equations of motion:

$$\Sigma(t)=\frac{\beta}{m}\frac{\alpha^2V_0}{d^4N}\sum_{\lambda}\langle\tilde{u}_\lambda(t),\tilde{u}_\lambda(0)\rangle, \tag{3.6}$$

where $\tilde{u}_\lambda$ is the coordinate of the λth eigenmode in the absence of the adatom. Note that $\Sigma(t)$, in this case, is simply the function $\eta(t)$, defined earlier in (2.11).[24,35] For phonons in the Debye model without the cutoff, the memory function is proportional to a delta function $\Sigma(t)=\eta\delta(t)$. Therefore its Fourier transform $\Sigma(\omega)$ is frequency independent, and there are no memory effects. The GLE, in this case, reduces to the simple Langevin equation.[16,17,34] When the cutoff of the Debye model is taken into account, $\Sigma(\omega)$ is frequency dependent even in the linear coupling model. In general, the real and imaginary parts of the Laplace transform of $\Sigma(t)$ are related, respectively, to the damping and the shift of the adatom energy.

For the case where $f_\lambda(x)$ is not a constant, two approximations have frequently been employed in the literature.[20,24] The first is the initial value approximation (IVA). This is valid when the substrate phonons time scale is much shorter than the adatom time scale. In this case, during a period of oscillation of the phonons, the particle has barely moved, so $\langle f_\lambda(x(t)),f_\lambda(x(0))\rangle$ can be replaced by $\langle f_\lambda(x(0))^2\rangle$, and $\Sigma(t)$ becomes

$$\Sigma_{\mathrm{IVA}}(t)=\frac{\beta}{m}\sum_{\lambda}\langle|f_\lambda(x(0))|^2\rangle\langle u_\lambda|\exp iQLQt|u_\lambda\rangle. \tag{3.7}$$

The expression for the memory function now does not contain explicitly the adatom variables, and the effect of nonlinear coupling is only to reduce its value by the temperature-dependent factor $\langle|f_\lambda(0)|^2\rangle$. As in the linear coupling case, the effect of the Liouville operator QLQ is to project out the adatom coordinate in the phonons equation of motion. For our choice of the coupling function, it is easy to see that $\Sigma_{\mathrm{IVA}}(t)$ reduces to the function $\eta(t)$ defined earlier in (2.11).

The generalized Langevin equation with the IVA approximation for the memory function has been studied anaytically with the matrix continued-fraction method.[24,30,31]. We will compare our molecular-dynamics simulations results with the corresponding analytic results in the next section.

The second common approximation for the memory function is the mode-mode coupling approximation. Here, one approximates the full memory function by the product of two distinct correlation functions, one for the adatom variables and the other for the substrate phonon variables. The memory function is then given as

$$\Sigma_{\mathrm{mod}}(t)=\frac{\beta}{m}\sum_{\lambda}\langle u_\lambda|\exp iQLQt|u_\lambda\rangle\langle f_\lambda(x(t)),f_\lambda(x(0))\rangle. \tag{3.8}$$

Changing the summation from λ to (i,l) and expressing the phonons coordinate correlation function in terms of $\eta(t)$, we obtain the expression

$$\Sigma_{\rm mod}(t)=\eta(t)\frac{d^4N}{\alpha^2V_0^2}\sum_{i=1,2}\langle f_i(x(t)),f_i(x(0))\rangle, \quad (3.9)$$

where $f_i(x)$, defined in (3.3), is independent of the index l. As stated earlier, in both the IVA and mode-mode coupling approximations, the memory function depends on the phonon excitations only through the function $\eta(t)$ defined earlier, and not on other details of the substrate. Even with the mode-mode coupling approximation to the memory function, the solution of the GLE is rather difficult since $\Sigma_{\rm mod}(\omega)$ still involes the adatom correlations function. The solution requires then iteration to self-consistency. So far, only limited results exist for specific models.[20,24] In order to compare our molecular-dynamics simulation results to the corresponding solution of the GLE in the mode-mode coupling approximation, we employ the following scheme. First, from our molecular-dynamics results, we can compute the correlation function for the adatom variable $\langle f_i(x(t))f_i(x(0))\rangle$. Together with the knowledge of the damping function $\eta(t)$ introduced earlier, this allows us to evaluate the $\Sigma_{\rm mod}(\omega)$ according to Eq. (3.1). We then introduce an effective Hamiltonian in which the adatom is coupled linearly to a set of substrate phonons. We choose the phonon parameters ω_λ and γ_λ, for this new problem such that the corresponding memory function in this linear coupling model, is equal to the mode-mode coupling memory function calculated from the nonlinear coupling under study. We then run a molecular-dynamics simulation for this effective linear coupling model. The comparison of the results from this second simulation with the original simulation results for the nonlinear model then allows us to gauge the accuracy of the mode-mode coupling approximation for the memory function. This comparison will be presented in the next section.

IV. RESULTS

In this section, we analyze the results obtained with MD in three different regimes, characterized by the ratio of the frequency of the adatom vibrational mode to the maximum substrate phonon frequency: $\omega_D=10\omega_0$, $\omega_D=\omega_0$, and $\omega_D=0.1\omega_0$.

Molecular-dynamics simulations are performed with an integration step of $0.05\ \omega_0^{-1}$ and a total number of 13 607 200 steps is used to obtain the results presented in this section. Long simulations are necessary to evaluate diffusion properties correctly. At low temperatures the jump rate is quite small and many steps are needed in order to obtain good statistics of the events.[40,41] Diffusive and vibrational properties are studied by evaluating the time dependent correlation functions defined in (2.9) and (2.10). Their Fourier transforms are calculated in an interval of 65 536 steps, in order to have a good resolution in frequency space.

A. Results for $\omega_D=10\omega_0$

This is the regime where most analytical work has been done and many theories have been developed to account for diffusive and vibrational properties of the adatom. Because of the rapid fluctuating force acting on the adatom due to the coupling to fast substrate phonons, we expect memory effects to be negligible and the results obtained from the solution of GLE with the IVA approximation should be very accurate.[22,24] Also, the cutoff in the phonon spectrum should have negligible effects and the IVA solution is therefore equivalent to a constant friction η in the Langevin equation.

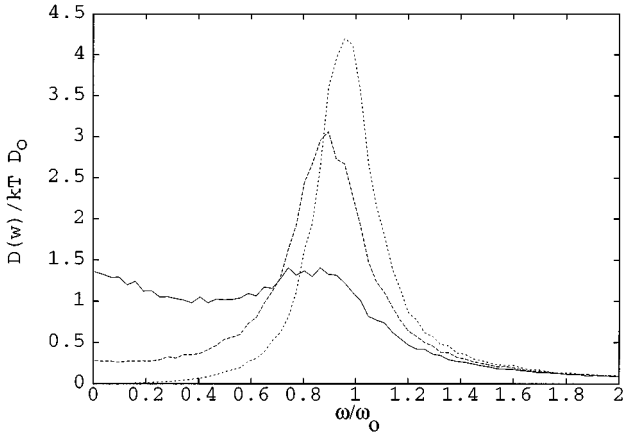

FIG. 2. Fourier transform of the velocity autocorrelation function $D(\omega)/k_BTD_0$ vs ω/ω_0 with $D_0=2\omega_0d^2$. Here $k_BT/V_0=0.2,0.5,1$ (dotted, dashed, and solid line, respectively) with $\omega_D=10\omega_0$ and $\eta/\omega_0=0.21$.

In Fig. 2, we plot the velocity autocorrelation function $D(\omega)$ vs ω, for several temperatures $k_BT=0.2,0.5,1V_0$ and with the friction parameter $\eta/\omega_0=0.21$. At low temperatures, a large vibrational peak, centered at $\omega\simeq\omega_0$, dominates the spectrum. To understand the mechanisms that contribute to the broadening of the vibrational peak, we have also evaluated the energy autocorrelation function. Its Fourier transform $E(\omega)$ has a Lorentzian peak centered at zero whose width is related to the rate of energy transfer between the adatom and the substrate excitations. In this case, we find that the value of the halfwidth at half maximum (HWHM) of the Lorentzian peak is equal to the width of the vibrational peak. This indicates that the main cause of broadening at low temperatures is through the decay of the adatom vibrational energy by transfer to the substrate excitations. At higher temperatures, the anharmonicity of the cosine potential starts to play an important role. The vibrational peak broadens further and the diffusive peak becomes dominant. Furthermore, as shown in Fig. 2, we observe a shift of the vibrational peak to lower frequencies as temperature increases. There are actually two competing effects contributing to the peak shift. First, the anharmonicity of the cosine potential changes the curvature of the potential well, allowing the existence of a wider spectrum of energy state, thus shifting the peak to lower frequencies. This effect is strongly temperature dependent. Second, the phonon-coupling produces a shift to higher frequencies.[10] The effect due to the anharmonic cosine potential dominates in this regime.

In Fig. 3, the diffusion constant is plotted as a function of inverse temperature for $\omega_D=10\omega_0$, $\omega_D=\omega_0$ and $\omega_D=0.1\omega_0$. The data for $\omega_D=10\omega_0$ shows that the diffusion process in this regime is thermally activated, with the diffusion barrier Δ simply equal to twice the amplitude of the cosine potential $2V_0$ as expected.[6]

In Fig. 4, we show a comparison between velocity autocorrelation function calculated using molecular dynamics and obtained solving analytically the GLE in the IVA

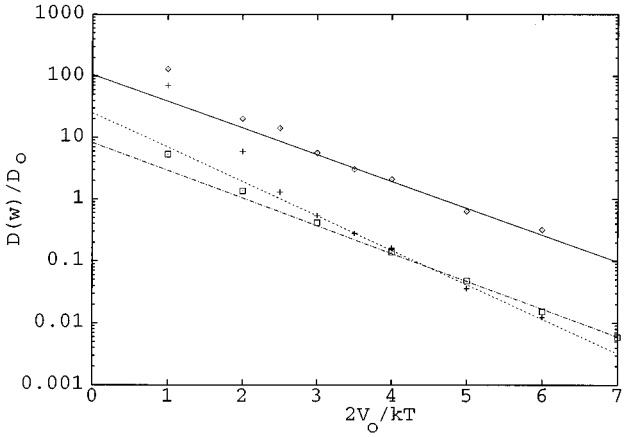

FIG. 3. Diffusion constant D/D_0 vs $2V_0/k_BT$ plotted in logarithmic scale with $D_0=\omega_0 d^2$; for $\omega_D=10\omega_0$ (squares), $\omega_D=\omega_0$ (plusses) and $\omega_D=0.1\omega_0$ (rhomboids). The slopes for straight line fitting the data are, respectively, -1.02 ± 0.03 for $\omega_D=10\omega_0$, -1.25 ± 0.05 for $\omega_D=\omega_0$, and -1.05 ± 0.1 for $\omega_D=0.1\omega_0$.

approximation.[22,24] These results are obtained for $\omega_D=10\omega_0$, $k_BT=0.2,0.333,0.5V_0$, and $\eta/\omega_0=0.21$. As expected, the results from the two calculations are almost identical in this regime provided we identify the value of $\eta(\omega=0)$ with the friction parameter η used in solving the GLE. Thus, in this regime, the IVA approximation provides an excellent description of the memory function and the effect of the cutoff in the phonon density of states is negligible. Furthermore, it is also an explicit demonstration that the scheme of using a few effective phonons is indeed able to describe the coupling to macroscopically large number of phonons provided that the phonon density of states is chosen to be the same in the two cases.

B. Results for $\omega_D=\omega_0$

In this regime the time scales of the adatom and the phonons are comparable and we do not expect IVA to be

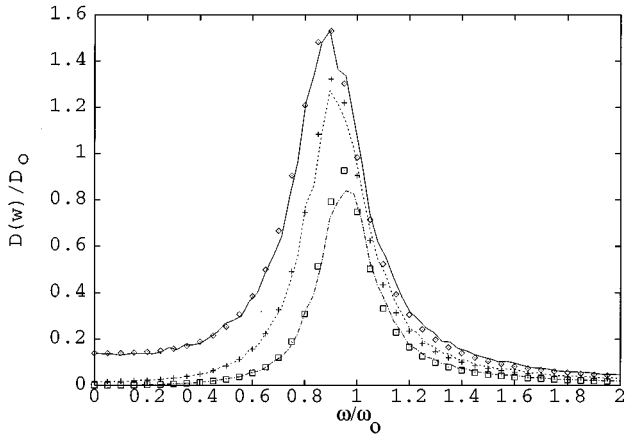

FIG. 4. Fourier transform of the velocity autocorrelation function $D(\omega)/D_0$ vs ω/ω_0 with $D_0=2\omega_0 d^2$. Lines are MD results, while symbols are the results from the analytical solution to GLE in the IVA approximation, using continued-fraction expansion. Curves for $k_BT/V_0=0.2,0.333,0.5$ (solid, dashed, and dashed-dotted, respectively) $\eta/\omega_0=0.21$ and $\omega_D=10\omega_0$.

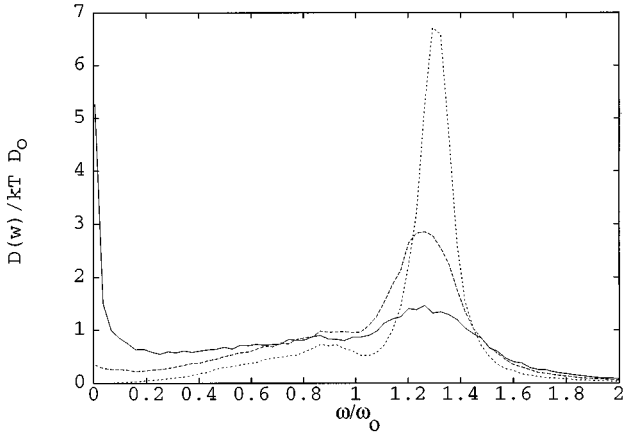

FIG. 5. Fourier transform of the velocity autocorrelation function $D(\omega)/k_BTD_0$ vs ω/ω_0 ($D_0=2\omega_0 d^2$). Here $k_BT/V_0=0.2,0.5,1$ (dotted, dashed, and solid line, respectively) with $\omega_D=\omega_0$ and $\eta/\omega_0=0.95$.

applicable here. Referring back to Fig. 3, we see that the diffusion constant D for $\omega_D=\omega_0$ still shows an Arrehnius activated form but with an effective diffusion barrier Δ equal to $2.5\pm0.05V_0$ insead of $2V_0$. The difference between the effective barrier and the adiabatic barrier $2V_0$ can be understood from the following reasoning. When the adatom sits in the well, it performs many oscillations before it attempts to jump, allowing therefore the substrate to relax. However the adatom crosses the barrier in a time interval of the order of $1/\omega_0$, which is comparable to the time scale of the substrate. Therefore the substrate does not have enough time to relax. Thus, the potential at the barrier is higher by approximately the magnitude of the relaxation energy which can be evaluated using (2.3) as

$$E_{\rm rel}=\frac{3\alpha^2V_0}{2d^2M\omega_D^2}, \tag{4.1}$$

where we have used the properties of the Debye model for the phonons. Indeed, we find that the difference $\Delta-2V_0$ and $E_{\rm rel}$ agree within our numerical uncertainty which is about 10%. In Fig. 5, we plot the velocity correlation function $D(\omega)$, for $k_BT=0.2,0.5,1V_0$, and $\eta/\omega_0=0.95$. At low temperatures, the vibrational peak dominates over the diffusive peak. In this regime, we notice that there is a significant blue shift of the vibrational peak. This is due to the strong level repulsion resulting from the coupling to substrate phonons. In fact, when the memory function is a step function, as resulting from the linear coupling to a Debye model phonons, the shift can be evaluated analytically as in (2.15).[10,24] The position of the vibrational peak is shifted to a new frequency $\tilde{\omega}$ given by

$$\tilde{\omega}\simeq\omega_0\sqrt{1-\frac{\eta}{\pi\omega_0}\ln\left|\frac{\omega-\omega_D}{\omega+\omega_D}\right|}. \tag{4.2}$$

As ω approaches ω_D, the shift diverges logarithmically. For the nonlinear coupling model under study, the shift is not divergent but still very large at ω close to ω_D. Besides this mechanism, the anharmonicity of the cosine potential causes a red shift in the opposite direction. The anharmonicity effect

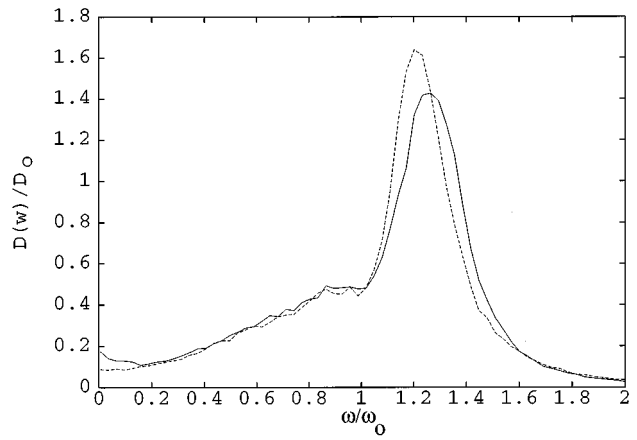

FIG. 6. Fourier transform of the velocity autocorrelation function $D(\omega)/D_0$ vs ω/ω_0 with $D_0=2\omega_0 d^2$. Solid curve represents tha exact numerical solution, the dashed curve has been obtained using the memory function in mode-mode coupling approximation. $k_BT/V_0=0.5$, $\eta/\omega_0=0.95$, and $\omega_D=\omega_0$.

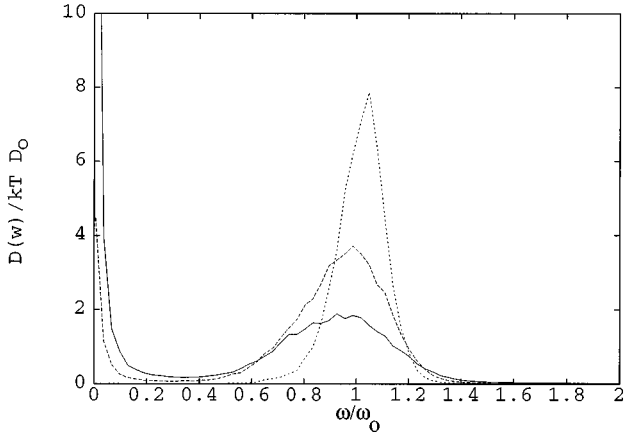

FIG. 7. Fourier transform of the velocity autocorrelation function $D(\omega)/k_BTD_0$ vs ω/ω_0 with $D_0=2\omega_0 d^2$. Here $k_BT/V_0=0.2,0.5,1$ (dotted, dashed, and solid line, respectively) with $\omega_D=0.1\omega_0$ and $\eta/\omega_0=2.2$.

gets stronger as the temperature increases but it is not sufficient to counterbalance the shift due to adatom-phonons coupling.

Examining the Fourier transform of the energy autocorrelation function, we found that $E(\omega)$ in this regime is not a simple Lorentzian. The energy decay, therefore, cannot be described by an unique time scale but it is more complex and involves several decay rates. The shape of the velocity autocorrelation function is also not a simple Lorentzian but it is asymmetric with a larger wing towards lower frequencies. It is clear, therefore, that when adatom and phonons time scales are comparable, memory effects are very strong and the simple picture of constant frictional damping is inadequate.

It is obvious that the IVA for the memory function breaks down here. We now want to compare our molecular-dynamics results with the corresponding solution of the GLE using the mode-mode coupling approximation for the memory function. We calculate $\Sigma_{\rm mod}(\omega)$ by evaluating first the adatom correlation function $\Sigma_{i=1,2}\langle f_i(x(t)),f_i(x(0))\rangle$, through our MD simulation results, and then substituting into Eq. (3.8) for $\Sigma_{\rm mod}(\omega)$. The memory function shows a strong temperature dependence and only approaches the IVA limit at low temperatures. As temperature increases the nonlinear part of the coupling becomes important so the zero-frequency value of $\Sigma_{\rm mod}(\omega)$ decreases and a large tail starts to form. Unlike the IVA, at high temperature, the sharp drop at $\omega=\omega_D$ has completely disappeared.

Figure 6 shows a comparison between velocity autocorrelation functions, obtained from the molecular-dynamics studies and the one obtained from solving the GLE in the mode-mode coupling approximation for $k_BT=0.5V_0$ and $\eta/\omega_0=0.95$. The two results are very similar. This indicates that the mode-mode coupling approximation gives a reasonably good description of the adatom dynamics in this regime. In particular, the diffusion motion is controlled by the friction $\eta=\Sigma_{\rm mod}(\omega\simeq 0)$. On the other hand, the adatom experiences a different damping whose strength is given by $\Sigma(\omega\simeq\omega_0)$ when it is vibrating in the well. The value of memory function at $\omega\simeq 0$ can differ significantly from the one at $\omega\simeq\omega_0$, when memory effects are important. Moreover, unlike the IVA limit, both $\Sigma_{\rm mod}(\omega\simeq 0)$ and $\Sigma(\omega\simeq\omega_0)$ are strongly temperature dependent. A qualitative trend indicates that as temperature increases the friction at zero frequency decreases, while its value at finite frequency increases.

C. Results for $\omega_D=0.1\omega_0$

In this regime, the adatom moves much faster than the phonons. In Fig. 7, we plot the velocity autocorrelation function for values of $k_BT=0.2,0.5,1V_0$ and for $\eta/\omega_0=2.2$. Here nonlinear coupling is essential for an understanding of the vibrational properties of the adatom. If the coupling between the phonons and the adatom were linear, the broadening of the vibrational peak would be dominated by effects of the anharmonic cosine potential, and the vibrational peak would approach a δ function at low temperatures.[10] However the nonlinear coupling enhances both the elastic and inelastic collision of the adatom with the substrate excitations and leads to finite broadening even at low temperatures. An analysis of the Fourier trasform of the energy autocorrelation function $E(\omega)$ shows that the HWHM of the Lorentzian peak is, in fact, more than an order of magnitude smaller than the width of the vibrational peak. This indicates that, in this regime, the coupling of the adatom to the substrate excitations results mainly in pure dephasing mechanisms, and the decay of the adatom vibrational energy due to the coupling to substrate excitations is negligible. At low temperatures, the dephasing due to the anharmonicity of the periodic potential is not important. Thus, the broadening mechanism here is due to the elastic dephasing events in the collision of the adatom with the substrate excitations.[43–45] In the quantum-mechanical regime, this would correspond to a multiphonon process resulting in no net energy transfer. These events would be too weak for the linear coupling model but they are strongly enhanced in the nonlinear coupling model.

Referring back to Fig. 3, we see that for $\omega_D=0.1\omega_0$, the diffusion constant again obeys the Arrenhius form with a barrier $\Delta=2.1\pm 0.1V_0$. The difference of Δ from the adiabatic barrier $2V_0$ can be understood again from the lack of substrate relaxation when the adatom is crossing the barrier.

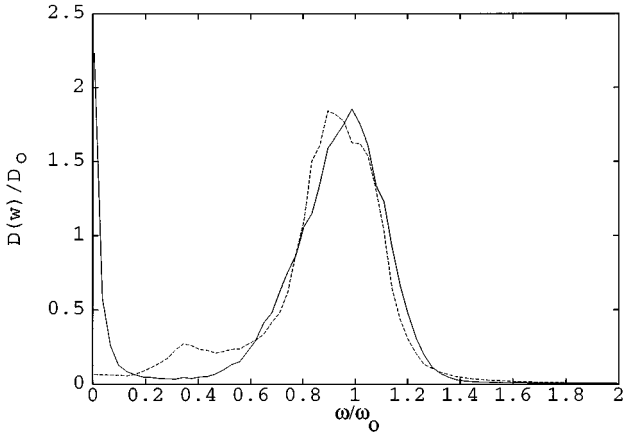

FIG. 8. Fourier transform of the velocity autocorrelation function $D(\omega)/D_0$ vs ω/ω_0 with $D_0=2\omega_0 d^2$. Solid curve represents tha exact numerical solution, the dashed curve has been obtained using the memory function in mode-mode coupling approximation. $k_BT/V_0=0.5$, $\eta/\omega_0=2.2$, and $\omega_D=0.1\omega_0$.

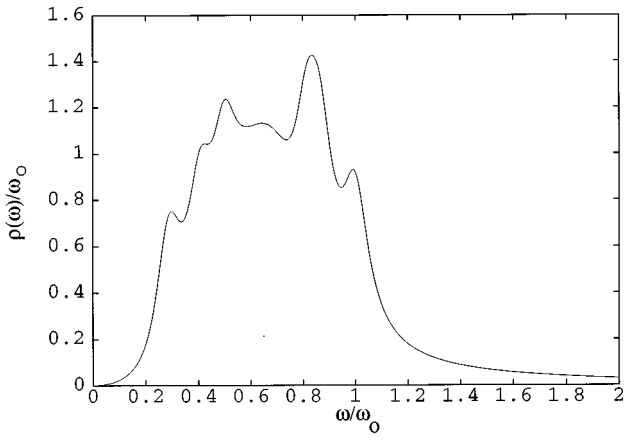

FIG. 9. The phonons density of states $\rho(\omega)/\omega_0$ vs ω/ω_0 with $\alpha=1$, $m=M=1$, and $\omega_s\simeq 0.85\omega_0$.

The prefactor D_0 here is more complicated than in the two regimes previously discussed. For example, the mode-mode coupling approximation predicts an effective friction at zero frequency $\eta_{\rm eff}(\omega\simeq 0)/\omega_0=1.3$ for $k_BT=0.5V_0$. This would lead to a result for D_0 according to the solution of the GLE of $D_0=3.5\omega_0 d^2$. Instead, we observe from the MD simulations a value of $D_0=121.8\omega_0 d^2$. The comparison shows that the numerical result for D_0 is, at least, an order of magnitude larger than the one obtained solving the GLE in mode-mode coupling approximation. This result extends at all temperatures and suggests that mode-mode coupling approximation is inadequte to describe the diffusive properties of the adatoms when its characteristic vibrational frequency is much faster than the substrate timescale.

It is important to stress that, in this regime, as in the case $\omega_D\simeq\omega_0$, the effective friction acting on the adsorbate is a frequency-dependent function. In its diffusive motion the adsorbate experiences a frictional force proportional to $\Sigma_{\rm mod}(\omega\simeq 0)$ while the damping is proportional to $\Sigma_{\rm mod}(\omega\simeq\omega_0)$ when the adatom vibrates in the well. Furthermore, when memory effects are important, the effective friction is also strongly temperature dependent. The memory function in the mode-mode coupling approximation $\Sigma_{\rm mod}(\omega)$ (3.8), only approaches the IVA value at low temperatures. As temperature rises, in fact the value of $\Sigma_{\rm mod}(\omega\simeq 0)$ decreases while $\Sigma_{\rm mod}(\omega\simeq\omega_0)$ increases. This indicates that, unlike the IVA limit, the contribution to the vibrational damping due to adatom-phonons coupling is not negligible.

Figure 8 shows a comparison between velocity autocorrelation functions, obtained through molecular-dynamics simulation studies, and the one in the mode-mode coupling approximation for $k_BT=0.5V_0$ and the phonons friction $\eta/\omega_0=2.2$. At finite frequencies, there is a reasonable agreement between the two results. The agreement, however, gets worse as $\omega\to 0$, leading to the difference in the value of the diffusion constant as discussed above.

D. Results beyond Debye model substrate phonons

All the results presented in the previous paragraphs have been obtained using substrate phonons characterized by Debye model. It is natural, therefore, to ask if the qualitative features of the diffusive and vibrational motion of the adatom change for more realistic models of substrate excitations. We discuss here briefly results obtained with molecular-dynamics simulation using a different model for the substrate phonons which contains more realistic features. In Fig. 9 we show the effective phonon density of state $\rho(\omega)$ adopted in this case. Referring to Eqs. (2.6) and (2.7), $\rho(\omega)$ is defined as

$$\rho(\omega)=\frac{2NM\omega^2}{\pi\Omega_0\alpha^2}\mathrm{Re}\,\eta(\omega), \tag{4.3}$$

where $\mathrm{Re}\,\eta(\omega)$ is the real part of the Laplace transform of $\eta(t)$ (2.18). As opposed to the Debye model, this new $\rho(\omega)$ now peaks in the middle of the spectrum and does not drop off to zero sharply at $\omega=\omega_D$. We now define a frequency ω_s as the frequency at which $\rho(\omega)$ reaches its maximum. The important parameter that determines the relation of the time scale of the adatom to that of the substrtate excitations is now the ratio $\gamma=\omega_s/\omega_0$. This now plays the role of the parameter ω_D/ω_0 defined earlier for the Debye model. We find again that the memory effects depend strongly on the ratio γ, with the IVA working well in the limit $\gamma\gg 1$, and the mode-mode coupling approximation reasonably well for $\gamma\leqslant 1$. All the qualitative features of the memory effects on the vibrational and diffusive motion of the adatom for different regimes of γ carries over to the new model. The only major difference is the frequency dependence of the friction in the IVA limit. For the Debye model in the IVA limit, the real part of $\eta(\omega)$ is proportional to the step function and the imaginary part is negligible for $\gamma\gg 1$. For the present model, while the imaginary part of $\eta(\omega)$ is still negligible, the real part of $\eta(\omega)$ is no longer a constant in the frequency region of interest but it is indeed strongly frequency dependent. This implies that the diffusive and vibrational motion are then controlled by different friction values $\eta(\omega\simeq 0)$ and $\eta(\omega\simeq\omega_0)$, respectively, instead of a single friction parameter η in the case of the Debye model.

V. CONCLUSIONS

In this paper, we have studied the diffusive and vibrational motion of an adatom coupled to substrate excitations

starting from a miscroscopic description of the system. We consider a coupling between the adatom and substrate phonons which is linear in the phonons coordinates but nonlinear in the adatom coordinate. We perform molecular simulation studies for this system with a small number of effective phonons. It is demonstrated that with proper choice of the frequency and damping of these effective phonons, the effect on the adatom is identical to that due to the interaction with a macroscopic number of substrate phonons in the thermodynamic limit. Our main focus is to analyze the memory effects of the frictional damping on the motion of the adatom.

We find that the importance of memory effects depends crucially on the parameter $\gamma=\omega_D/\omega_0$, with ω_D representing the Debye frequency of the substrate phonons and ω_0 the adatom vibrational frequency. In the limit $\gamma\gg 1$, the memory effects are largely negligible. In this case, we can identify a constant friction parameter η related to the zero-frequency limit of the phonon correlation function in our model. To better understand our numerical results, we can compare them with results obtained from a different but equivalent analytic approach. Starting from our microscopic model, we can derive a generalized Langevin equation (GLE) describing the motion of the adatom.[32,34–36] The effect of adatom-phonon coupling is contained in the memory function and a fluctuating random force in the GLE. When $\gamma\gg 1$, the memory function can be approximated in the initial value approximation[20,24] (IVA) and the GLE then can be solved by the matrix continued fraction method.[24,30,31] Our numerical results for the diffusion constant and the vibrational motion of the adatom are in excellent agreement with the IVA solution of the GLE. Thus we have demonstrated explicitly the validity of the IVA in the limit where the time scale of the substrate excitations is much shorter than that for the motion of the adatom.

When γ is comparable or much smaller than 1, memory effects start to manifest themselves. First, the vibrational peak begins to deviate from a pure Lorentzian shape because of the frequency dependence of the frictional damping. Also, the mechanism through which the adatom phonon coupling contribute to the vibrational lineshape broadening changes. For $\gamma\gg 1$, the line broadens mainly through the decay of the adatom vibrational energy via transfer to the substrate excitations. As γ increases, the broadening becomes dominated by pure dephasing effects due to the elastic collision of the adatom with the substrate phonons. Another manifestation of the memory effect is the shift in the vibrational peak frequency. Unlike the anharmonicity of the potential which always causes a red shift and is strongly temperature dependent, the frequency dependence of the frictional damping gives rise to a blue shift of the vibrational peak to higher frequencies. This shift peaks at the value of $\gamma\simeq 1$ as easily understood from the usual Kramer-Kronig analysis.[16,17]

The memory effects also affect strongly the diffusion properties. At low temperatures, we find the diffusion constant to obey an Arrehnius-activated form independent of the value of γ. However, starting at $\gamma\simeq 1$ and for $\gamma<1$, the value of the barrier gets renormalized by the adatom phonon coupling and becomes appreciably larger than the static barrier $2V_0$. In fact, while at the well the adatom oscillates for many periods before attempting to jump, allowing the substrate to relax. At the saddle the time necessary for the adatom to cross is very short compared to the time needed for the substrate to relax. As a consequence, the effective barrier is increased by the amount of the energy relaxation at the saddle. This analytical prediction agrees with the numerical result within 10%. This is in strong contrast to the Markovian limit where the adatom substrate coupling leads to a constant friction which only affects the prefactor in the Arrhenius form but not the barrier itself. As far as the prefactor is concerned, it is now controlled by an effective friction which is different from the finite frequency value contributing to the broadening of the vibrational line. This effective friction depends now not just on the phonon properties of the substrate but also on the adatom motion itself.

As discussed earlier, there is a GLE associated with the model we use in our molecular-dynamics simulation study. In the regime $\gamma<1$, the IVA for the memory function is no longer valid. The commonly used approximation in this regime, to incorporate memory effects in the solution of the GLE, is the so-called mode-mode coupling approximation. In the context of application to adatom dynamics, there have not been too many studies using this approach because of the complexities in its actual implementation. Unlike the IVA, the accuracy of the mode-mode coupling approximation for the memory function is more difficult to gauge. Our molecular-dynamics results allows us to determine the accuracy of the mode-mode coupling approximation for adatom dynamics. We find that over the wide frequency regime that we have studied, (γ ranging from 1 to 0.1) the correlation functions obtained from the GLE in the mode-mode coupling approximation agrees well with the exact numerical result in the finite frequency region of the spectrum. Thus, it is a good approximation for the study of the vibrational properties of the adatom. In the low-frequency region, the mode-mode coupling results start to deviate significantly from the molecular-dynamics results for $\gamma\ll 1$. This has a strong implication on the value of the diffusion constant, which can be expressed as the zero-frequency transform of the velocity autocorrelation function. For example, we find that for $\gamma=0.1$, the value of the diffusion constant obtained from the numerical simulation is more than an order of magnitude larger than the corresponding value from solving the GLE with the mode-mode coupling approximation. We expect that the qualitative features of our model will carry over to more complicated systems. Thus we conclude that while the mode-mode coupling approximation can be used with confidence for studying adatom vibrational dynamics, its application to surface diffusion can be problematic.

APPENDIX

In this appendix we derive the form of the coupling function, as given in Sec. II, from a pair potential interaction between the adsorbate and the substrate atoms. Let us assume that potential experienced by the adsorbate due to all the atoms on the lattice is

$$V_{\rm tot}(x)=\sum_j W(x\hat{x}-\mathbf{R}_j)=\sum_{j,\mathbf{k}} W(\mathbf{k})e^{i\mathbf{k}\cdot(x\hat{x}-\mathbf{R}_j)} \quad \text{(A1)}$$

where x is the adatom coordinate and $\mathbf{R}_j$ is the coordinate of the substrate atoms characterized by the index j. In the har-

monic approximation $\mathbf{R}_j=\mathbf{R}_j^0+\mathbf{u}_j$, where $\mathbf{R}_j^0$ is the equilibrium position of the atom in the lattice and $\mathbf{u}_j$ is the displacement from the equilibrium position such that $\mathbf{u}_j \ll \mathbf{R}_j$. Then $V_{\rm tot}(x)$ to lowest order in $\mathbf{u}_j$ can be rewritten as

$$V_{\rm tot}(x)=\sum_{j,\mathbf{k}} W(\mathbf{k})e^{i\mathbf{k}\cdot(x\hat{x}-\mathbf{R}_j^0)}-\sum_{j,\mathbf{k}} W(\mathbf{k})e^{i\mathbf{k}\cdot(x\hat{x}-R_j^0)}i\mathbf{k}\cdot\mathbf{u}_j. \tag{A2}$$

The total potential consists of two parts. The first is the static potential generated by the lattice atoms in their equilibrium position and in our model is approximated by a cosine potential. The second depends on $\mathbf{u}_j$, therefore on the dynamics of the substrate and it corresponds to the interacting part of the Hamiltonian described in (2.4).

Focusing on the second term, we rewrite the wave vector $\mathbf{k}=\mathbf{q}+\mathbf{G}$ where $\mathbf{q}$ is restricted to the first Brillouin zone, while $\mathbf{G}$ are the reciprocal-lattice vectors. Since $\exp(-i\mathbf{G}\cdot\mathbf{R}_j^0)=1$ $V_{\rm int}$ becomes

$$V_{\rm int}(x)=-i\sum_{j,\mathbf{q},\mathbf{G}} W(\mathbf{q}+\mathbf{G})e^{i(q_x+G_x)x}(\mathbf{q}+\mathbf{G})\cdot\mathbf{u}_j e^{-i\mathbf{q}\cdot\mathbf{R}_j^0}. \tag{A3}$$

Noting that $\Sigma_j \mathbf{u}_j e^{-i\mathbf{q}\cdot\mathbf{R}_j^0}$ is just the Fourier component $\mathbf{u}_\mathbf{q}$, then

$$V_{\rm int}(x)=-i\sum_{\mathbf{q},\mathbf{G}} W(\mathbf{q}+\mathbf{G})(\mathbf{q}+\mathbf{G})\cdot\mathbf{u}_\mathbf{q}\{\cos[(q_x+G_x)x] + i\sin[(q_x+G_x)x]\}. \tag{A4}$$

Furthermore, restricting the summation of $\mathbf{q}$ to half spin

$$V_{\rm int}(x)=-i\sum_{\mathbf{q},\mathbf{G}}{}' (\mathbf{q}+\mathbf{G})\cdot\{[\mathbf{u}_\mathbf{q}W(\mathbf{q}+\mathbf{G}) - \mathbf{u}_{-\mathbf{q}}W(-\mathbf{q}-\mathbf{G})]\cos[(q_x+G_x)x] + i[\mathbf{u}_\mathbf{q}W(\mathbf{q}+\mathbf{G})+\mathbf{u}_{-\mathbf{q}}W(-\mathbf{q}-\mathbf{G})] \times\sin[(q_x+G_x)x]\}. \tag{A5}$$

Substituting for $\mathbf{u}_\mathbf{q}=(\mathbf{u}_{1,\mathbf{q}}+i\mathbf{u}_{2,\mathbf{q}})/\sqrt{2}$ and $\mathbf{u}_{-\mathbf{q}}=\mathbf{u}_\mathbf{q}^\star$ and assuming that $W(\mathbf{q}+\mathbf{G})=W(-\mathbf{q}-\mathbf{G})$, then

$$V_{\rm int}(x)=\sqrt{2}\sum_{\mathbf{q},\mathbf{G}}{}' W(\mathbf{q}+\mathbf{G})(\mathbf{q}+\mathbf{G})\cdot\{\mathbf{u}_{1,\mathbf{q}}\sin[(q_x+G_x)x] + \mathbf{u}_{2,\mathbf{q}}\cos[(q_x+G_x)x]\}. \tag{A6}$$

The specific coupling that we have choosen for our simulations retains some of the features of the general coupling derived here. It can be regarded as an approximation to $V_{\rm int}(x)$ when the function $W(\mathbf{q}+\mathbf{G})$ peaks sharply at $\mathbf{q}+\mathbf{G}=(2\pi/a)\hat{x}$. Replacing the $\mathbf{q}$ label by the general index l, the coupling can then be written as

$$V_{\rm int}(x)=A\sum_l [u_{1,l}\sin(x/d)+u_{2,l}\cos(x/d)], \tag{A7}$$

where $A=\alpha V_0/(d\sqrt{N})$ and $d=a/2\pi$.

ACKNOWLEDGMENTS

We thank Professor Liao Chen for many helpful discussions. This work is supported in part through an ONR grant.

[1] R. Gomer, Rep. Progr. Phys. **53**, 917 (1990).
[2] R. G. Tobin, Surf. Sci. **183**, 226 (1987).
[3] H. Ueba, Prog. Surf. Sci. **22**, 181 (1986).
[4] G. Wahnström, in *Interaction of Atoms and Molecules with Solid Surfaces*, edited by V. Bertolani, N.H. March, and M.P. Tosi (Plenum, New York, 1990), p. 529.
[5] T. Ala-Nissila and S. C. Ying, Prog. Surf. Sci. **39**, 227 (1992); Phys. Rev. B **42**, 10 264 (1990).
[6] H. A. Kramers, Physica **7**, 284 (1940).
[7] V. P. Zhdanov, Surf. Sci. **214**, 289 (1989).
[8] E. Pollak, J. Bader, B. J. Berne, and P. Talkner, Phys. Rev. Lett. **70**, 3299 (1993).
[9] R. Ferrando, R. Spadacini, and G. E. Tommei, Phys. Rev. E **48**, 2437 (1993).
[10] J. W. Gadzuk and A. C. Luntz, Surf. Sci. **144**, 429 (1984).
[11] J. A. Leiro and M. Persson, Surf. Sci. **207**, 473 (1989).
[12] O. M. Braun, Surf. Sci. **213**, 336 (1989).
[13] A. I. Volokitin, O. M. Braun, and V. M. Yakovlev, Surf. Sci. **172**, 31 (1986).
[14] A. I. Volokitin, Surf. Sci. **224**, 359 (1989).
[15] P. Hänggi, P. Talkner, and M. Borkovec, Rev. Mod. Phys. **62**, 251 (1990).
[16] H. Risken, *The Fokker Planck Equation* (Springer-Verlag, Berlin, 1984).
[17] D. Foster, *Hydrodynamic Fluctuations, Broken Symmetry and Correlation Functions* (Benjamin, New York, 1975).
[18] E. Pollak, J. Chem. Phys. **85**, 865 (1986).
[19] R. Ferrando, R. Spadacini, and G. E. Tommei, Surf. Sci. **265**, 273 (1992); **251**, 773 (1991); **269**, 184 (1992).
[20] G. Wahnström, Surf. Sci. **159**, 311 (1985).
[21] G. Wahnström, Surf. Sci. **164**, 449 (1985); Phys. Rev. B **33**, 1020 (1986).
[22] L. Y. Chen and S. C. Ying, Phys. Rev. Lett. **71**, 4361 (1993).
[23] L. Y. Chen and S. C. Ying, Phys. Rev. B **49**, 13 838 (1994).
[24] L. Y. Chen and S. C. Ying, J. Electron. Spectrosc. **64**, 797 (1993).
[25] R. Ferrando, R. Spadacini, G. E. Tommei, and A. C. Levi, Physica A **173**, 141 (1991).
[26] B. Carmeli and A. Nitzan, Phys. Rev. Lett. **29**, 1481 (1984).
[27] J. Ellis and R. J. Toennies, Phys. Rev. Lett. **70**, 2118 (1993).
[28] F. Hofmann and R. J. Toennies (unpublished).
[29] M. F. Bertino, F. Hofmann, W. Steinhögl, and R. J. Toennies (unpublished).
[30] S. C. Ying, Phys. Rev. B **41**, 7068 (1990).
[31] H. Mori, Progr. Theor. Phys. **34**, 399 (1965).
[32] C. Caroli, B. Roulet, and D. Saint-James, Phys. Rev. B **18**, 545 (1978).
[33] P. Mazur, and I. Oppenheim, Physica **50**, 241 (1970).
[34] A. O. Caldeira and A. J. Leggett, Ann. Phys. **149**, 374 (1983).
[35] E. Cortes, B. J. West, and K. Lindenberg, J Chem. Phys. **82**, 2708 (1985).

[36] E. Pollak, A. M. Berezhkovskii, and Z. Schuss, J. Chem. Phys. **100**, 334 (1994).
[37] K. Lindenberg and E. Cortes, Physica **126 A**, 489 (1984).
[38] K. Lindenberg and V. Seshadri, Physica **109 A**, 483 (1981).
[39] M. Bianucci and P. Grigolini, J. Chem. Phys. **96**, 6138 (1992).
[40] M. P. Allen and D. J. Tildesley, *Computer Simulation of Liquids* (Clarendon, Oxford, 1987).
[41] D. W. Heerman, *Computer Simulation Methods in Theoretical Physics* (Springer, Berlin, 1986).
[42] J. C. Tully, J. Chem. Phys. **73**, 1975 (1980).
[43] B. N. J. Persson and R. Ryberg, Phys. Rev. B **32**, 3586 (1985).
[44] S. Marks, P.A. Cornelius, and C. B. Harris, J. Chem. Phys. **73**, 3069 (1980).
[45] R. M. Shelby, C. B. Harris, and P. A. Cornelius, J. Chem. Phys. **70**, 34 (1979).